PROBING COSMIC INFLATION: TESTING NOVEL HIGH-SENSITIVITY DETECTORS FOR NEXT-GENERATION SURVEYS

Jordan E. Shroyer
Advisor: Dr. Bradley R. Johnson
Department of Astronomy, University of Virginia

April 11, 2023

Abstract

Next-generation cosmological surveys will require detectors with unprecedented sensitivity that can measure the faint "relic radiation" of the early universe. This "relic radiation," also known as the cosmic microwave background, exhibits faint patterns which reveal how the universe expanded just after the Big Bang. Kinetic inductance detectors are an emerging technology that is well-suited for measuring very faint signals. Our group uses a novel detector design—multichroic microwave kinetic inductance detectors—which is sensitive to two frequency ranges simultaneously. The ability to simultaneously observe at multiple frequencies facilitates the efficient removal of contaminating foreground sources from the data, which is necessary to recover the signal of interest. I am currently testing the performance of prototype detector arrays to demonstrate their suitability for next-generation surveys. This paper describes our prototype arrays and discusses the experimental system. I highlight the development and validation of the readout system I built, which I will use to measure how the detectors respond to light. I also describe the experimental setup and optical tests I will use to characterize the performance of the detector arrays. Each component of the system is complete and validated, so we are ready to begin testing the prototype detector arrays.

1 Introduction

The core goal of cosmology is to determine how the structure and composition of the Universe have evolved through time. The leading theory proposes a period of rapid, exponential expansion of space just after the Big Bang, i.e. an "epoch of inflation." Inflation would leave observable evidence: a characteristic pattern of polarization fluctuations across the sky nicknamed "B-modes." (See Fig. 1.) Inflation is predicted to generate gravitational waves, causing characteristic B-mode fluctuation patterns in the light emanating from the very early universe.[7] This light from the early universe is known as the cosmic microwave background (CMB), sometimes called "relic radiation" or the "afterglow of the Big Bang." Maps of the CMB encode a wealth of information about conditions in the early universe. Observations of another polarization pattern, "E-modes," along with brightness fluctuations have been used to determine properties like curvature, initial conditions, and particle abundances through the history of the Universe.[7] Observing B-modes would be exceptional evidence for the theory of inflation.

To date, however, B-modes have not been detected. State-of-the-art detectors have already reached the statistical noise limit on sensitivity, and have constrained the B-mode polarization level to one part in one hundred thousand.[7] If B-modes exist, detecting

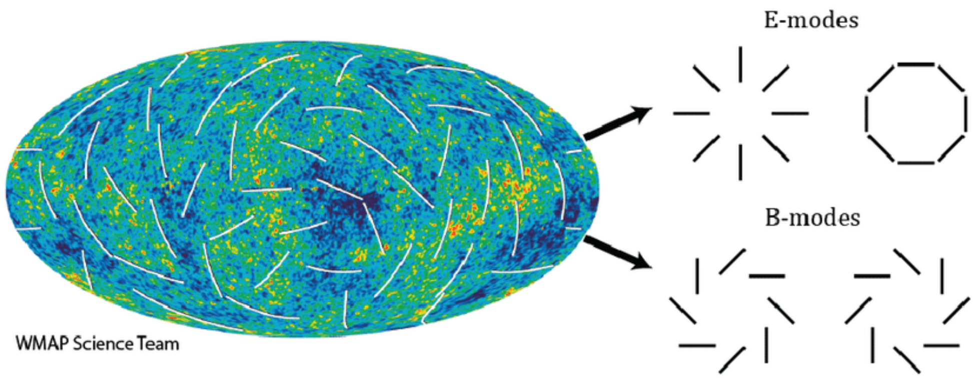

Figure 1: Map of the cosmic microwave background illustrating polarization fluctuations across the sky. The names "E-mode" and "B-mode" describe the linear polarization patterns and are essentially mnemonics, chosen because the patterns are reminiscent of electric (E) and magnetic (B) field shapes. E- and B-modes are observer independent. In the 2D flat-sky limit, they are analogous to Stokes Q and U, respectively. Figure from [4].

them will require greater sensitivity, which will be achieved with larger detector arrays.

B-mode detection is further complicated by the objects and dust from the Galaxy appearing the foreground of the CMB maps. When these foreground sources emit polarized light, they contaminate CMB polarization patterns, potentially being mistaken for the B-modes produced by inflation.[1, 6] Future surveys will therefore require sophisticated foreground removal, which will be aided by multi-chroic detectors, which simultaneously measure foregrounds and the CMB across a range of frequencies. Multichroic observing will not only enhance CMB studies, but also provide valuable all-sky survey data for galactic scientists, because the "contaminants" in our CMB maps are their science targets.[2]

This paper discusses our experimental design to test the performance of a novel detector technology designed to study CMB polarization with unprecedented sensitivity; our detector arrays simultaneously measure CMB and foreground signals to facilitate removal of contaminant signals. The goal of the experiment is to measure sensitivity and noise levels of various prototype arrays of multi-chroic microwave kinetic inductance detectors (MKIDs). Additionally, we want to measure the polarization response of the detectors. If the prototype arrays perform as well as anticipated, these detectors will pave the way for the construction of larger arrays for future surveys.

2 System Overview

I am testing novel detectors that are optimized for CMB polarization measurements. Our detectors are housed inside an aluminum enclosure, described in Section 2.1. The enclosure is designed to optimize the coupling between the detectors and the sky signal. Section 2.2 describes the KID technology in general and the specific architecture used for our prototype arrays. The detectors are made from superconducting materials ($T_c = 1.4$ K), and are therefore cryogenically cooled using the system outlined in Section 2.3. Section 2.4 describes the optical testing setup I will use to characterize the detectors. Finally, Section 2.5 describes the readout system, which is used to send signals into the cryostat to operate the detectors, monitor the detector response from outside the cryostat, and log the data on a computer.

2.1 Aluminum Enclosure Modules

The detector array is mounted inside an aluminum enclosure. Incident radiation enters the module through the top of the enclosure, by coupling to the horn array (see Figure 2, upper panel.) Each opening in the array is a feedhorn antenna. Directly below each horn is one “pixel” of the detector array. In the lower panel of Figure 2, the top of the enclosure has been removed so that the 23-pixel MKID array is visible. On the right-hand side of the module in the photo, there are two SMA connectors. The detectors are monitored using a “probe tone” which enters the module through one SMA cable, meanders around the wafer to pass by each MKID, and exits the module through the other SMA cable. The probe tone is controlled using the readout system described in section 2.5.

2.2 Detectors

I am characterizing multi-chroic microwave kinetic inductance detectors (MKIDs.) MKIDs are being developed for a variety of applications and wavelengths. Ours are optimized for CMB observations. Kinetic inductance detectors are photon-sensitive superconducting resonators. Figure 3 shows a single pixel in our detector array consisting of four MKIDs (drawn in red and blue).

To make more sensitive observations of the CMB, larger detector arrays are necessary. This is challenging because the state-of-the-art detectors, TES bolometers, must be operated in a cryostat at sub-kelvin temperatures to function. Larger bolometer arrays require additional wires to record data from the detectors. Each additional wire conducts heat into the cryostat, so bolometer arrays are limited to ∼64 elements to keep thermal loading acceptably low.[7] The underlying physics of MKIDs makes them naturally well-suited for use in large detector arrays because when each detector is assigned a unique resonant frequency, the data can be read out with a single transmission line. MKIDs are also operated at sub-kelvin temperatures, but a single pair of SMA cables (Fig. 2) can carry a superposition of probe tones to simultaneously monitor every detector in the array. This reduces thermal loading compared to TES bolometers. In principle, MKID arrays can have thousands of elements. Other kinetic inductance detectors (KIDs) with different designs have been developed, and array sizes of ∼250 detectors

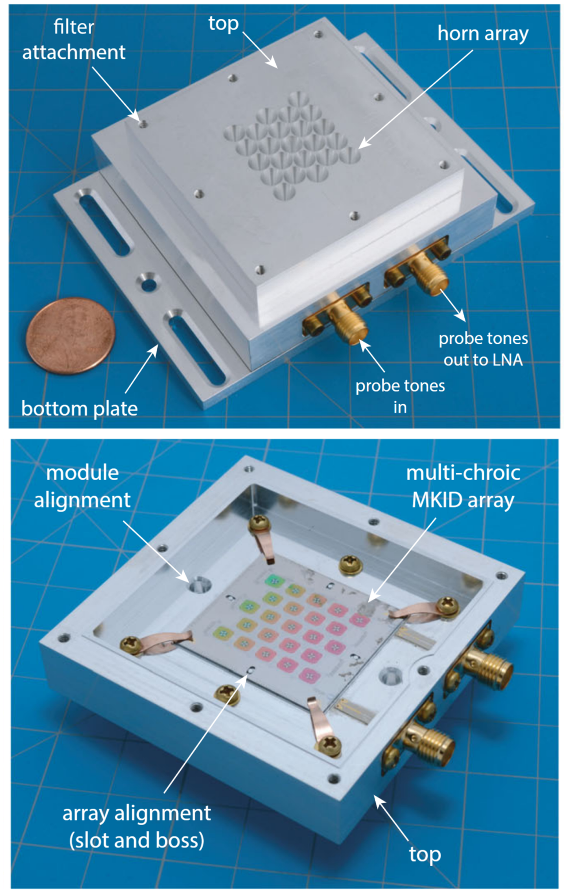

Figure 2: **Top:** 23-element array of multichroic detectors in aluminum enclosure. The horn array couples to incident light and transmits it to the detectors inside. **Bottom:** Each horn in the array sits above an array element consisting of four detectors, each sensitive to one of the two frequency bands and one of two polarization orientations. Together the array element is sensitive to orthogonal polarization in both spectral bands. Figures from [3].

have been achieved, but KIDs have yet to be used for CMB observations.[7]

We are working with multi-chroic MKIDs. By definition, multi-chroic detectors are sensitive to two or more frequency bands. Our detectors are sensitive to two frequency bands, centered on the peak of the CMB spectrum (150 GHz) and on Galactic dust emission where it exceeds CMB emission (235 GHz) [3]. This means that our detectors will be sensitive to both CMB emission and dust emission, facilitating the sophisticated foreground removal needed for future high-sensitivity B-mode searches.

There are two sets of relevant frequencies in this discussion. First is the frequency of the sky signal measured by the detector (150 and 280 GHz). Any photons of sufficient energy are capable of breaking Cooper pairs in the aluminum, so we use the band-pass filters to select only the frequencies of interest. Next is the resonant frequency of each detector (3-5 GHz). The resonant frequencies of the detectors are chosen based on the resolution and bandwidth of the readout system. The goal is to pack the resonant frequencies as closely as possible, without overlap.

Figure 3 is a schematic diagram of a single array "pixel," which corresponds to one of the squares below a feedhorn in Figure 2. The gray circle in the center outlines the feedhorn profile. Incident radiation hits the green paddles in the center—the orthomode transducer (OMT). The OMT is connected to the octagonal transmission line, which features "stubs" around the interior edge that filter the radiation before it enters one of four hybrid tees. Each hybrid tee receives one polarization in one of the two spectral bands. The slotline transition couples the signal to the aluminum sensing element.

Our MKIDs consist of two sections, an aluminum sensing element to absorb the radiation and the larger niobium-over-

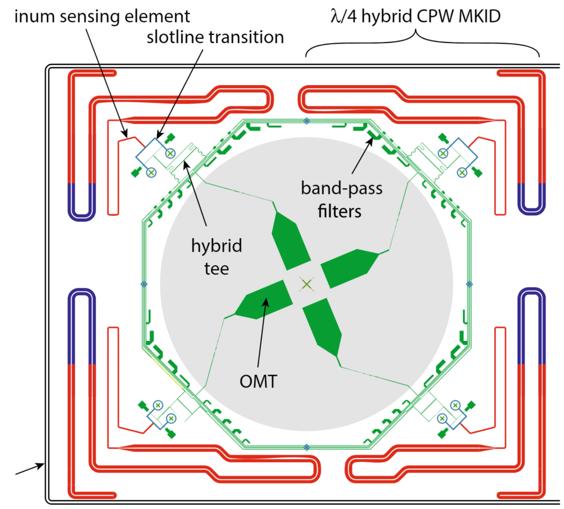

Figure 3: A single array element with four detectors. Radiation couples to the OMT, passes through the band-pass filter, and couples to the resonators. Cooper pairs break in the aluminum sensing element, shifting the resonance frequency. Each resonator in the array is assigned a unique frequency by adjusting the length of the $\lambda/4$ hybrid CPW MKID, allowing all detectors to be read out unambiguously on a single transmission line. Figure from [3].

aluminum bilayer section, where the length is tuned so that each MKID resonates at a unique frequency. When photons are absorbed in the aluminum sensing element, they break Cooper pairs and increase the kinetic inductance of the material. The MKID can be modeled as an RLC circuit, with resonant frequency f_0 and quality factor Q defined as

$$f_0 = \frac{1}{2\pi}\frac{1}{\sqrt{LC}}, \tag{1}$$

$$Q = \frac{1}{R}\sqrt{\frac{L}{C}}. \tag{2}$$

The inductance L is the sum of the geometric inductance L_g and the kinetic inductance L_k, so when L_K increases f_0 decreases and Q increases. This corresponds to a frequency down shift and broadening of the resonance peak. We detect this shift as a change in the amplitude and phase of the probe tone.

2.3 Cryogenic System

The absorbing section of the detectors is made of aluminum, with a critical temperature T_c of 1.4 K. We test the detectors at about $T_c/10$. Our cryogenic system reaches sub-kelvin temperatures. The system is cooled to 3 K using a Cryomech PT407 pulse tube cooler (PTC), and achieves sub-kelvin temperatures with a two-stage adiabatic demagnetization refrigerator (ADR). The top panel of figure 4 is a photograph of the cryostat set up for testing. The bottom panel of Figure 4 is a photograph of the lower section of the cryostat. The vacuum shells and radiation shields have been removed, exposing the experimental stages inside.

2.4 Optical Testing Setup

To test the arrays, I will follow similar methods to [5], which analyzes another KID architecture. My optical characterization measurements will focus on characterizing the sensitivity and low-frequency noise of the detectors. I have prepared the sub-kelvin cryostat in our lab at UVA for testing (Figure 4). The first two tests will be "dark measurements," conducted with no illumination on the array. The remaining tests will use three components: a variable blackbody source (tests 3, 5), electronic millimeter-wave sources producing broadband or continuous radiation centered on 150 GHz and 235 GHz (tests 4, 5), and a rotating half-wave plate (test 6). The testing setup is shown in Figure 4. Planned tests include:

1. **Identify resonance frequencies.** We will sweep the probe tone through the nominal frequency range of the resonators, measuring the time-ordered spectral response of the complex scattering parameter S_{21}. "Dips" in the $|S_{21}|^2$ versus frequency spectrum indicate resonance frequencies.

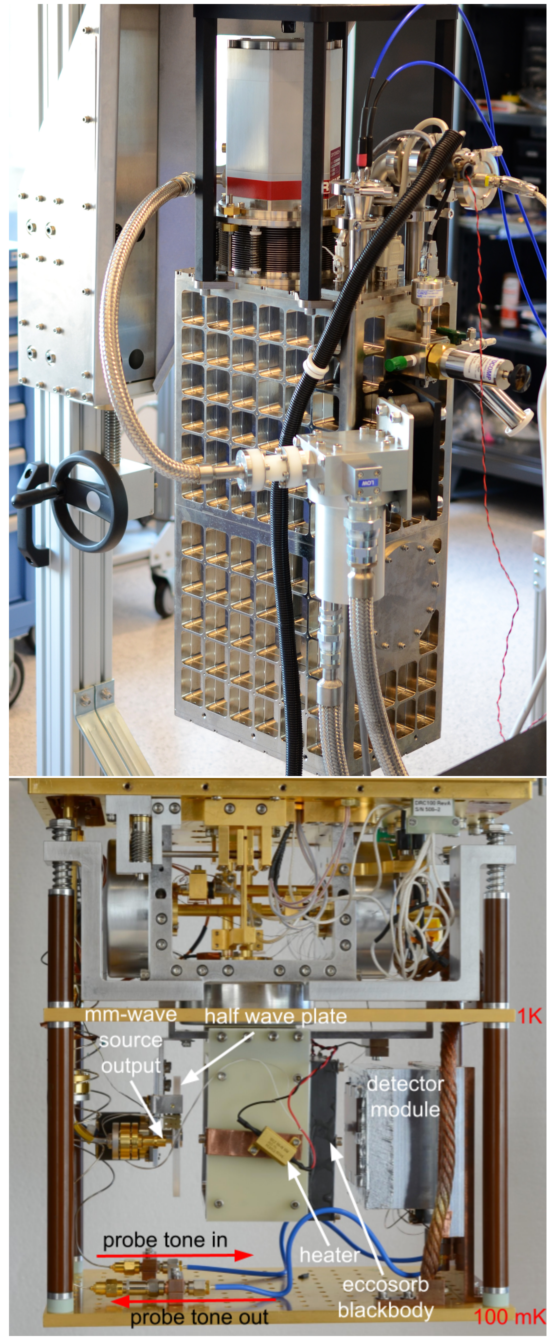

Figure 4: Photo of the experimental setup for optically characterizing the detector array. On the far left, the mm-wave source output passes through the rotatable half-wave plate, then through the eccosorb blackbody. These components are all attached to the stage labeled "1K." The detector module is mounted vertically on the 100mK stage to the right-hand side of the photo. At the bottom, the cable labeled "probe tone in" carries the probe tone from the room-temperature readout system (section 2.5) into the cryostat and to the detector module. The cable labeled "probe tone out" carries the probe tone out of the detector module, out of the cryostat, and back to the readout system.

2. **Characterize resonator quality factors.** We send the superposition of the previously identified resonance frequencies (i.e. the probe tone) to the detectors via the transmission line. I will use the readout system to monitor the transmission line output, measuring the S_{21} response under various temperature and illumination conditions. I will determine the resonator quality factors by fitting a model to the S_{21} data.

3. **Calibrate resonators.** To map detector response to a physical temperature, I will illuminate the array with the variable blackbody source and record the detector responses to changing source temperature.

4. **Test spectral response.** Since the blackbody source varies slowly, it cannot reveal spectral response times. So, to find the frequency response time and sensitivity range, I will switch the mm-wave source on and off at varying frequencies until we find the limits. The response time limits how quickly data can be collected, and therefore sets the required observing time.

5. **Determine noise properties.** The noise spectra are found by taking the power spectral density (PSD) of the test 2 results I will calibrate to units of $\mathrm{mK}/\sqrt{\mathrm{Hz}}$ using the results of test 1.

6. **Measure polarization response.** The thickness of the rotating half-wave plate is tuned so the E_x, E_y components of incident waves are 90° out of phase. At any orientation, the detectors measure Stokes I plus some fraction of Q and U. By rotating the plate 360° and using a model to demodulate the data, one detector can measure the full Stokes parameters.

2.5 Readout System

I built and programmed the readout system we will use to test our detector arrays. This is a homodyne system, so it produces only one frequency at a time, and therefore can only be used to characterize one detector at a time. We would not operate the MKIDs this way in a real astronomical observing context, but it is useful for characterizing prototype array. The homodyne system is simpler, and in principle the system noise is easier to understand. The homodyne readout system is therefore advantageous for a detailed characterization of individual resonators, which is our objective in testing the detector design. The readout system operates at room temperature. It generates a sinusoidal "probe tone." The probe tone is routed into the cryostat, through the detector array, and back out of the cryostat. The detectors modulate the probe tone; by comparing the modulated probe tone to the original we can measure the detector response.

Hardware. We selected an ADC with a high sample rate and the ability to continuously collect data for an arbitrarily long time. It is important to have sufficiently high spectral resolution at the frequencies where the MKID noise features are expected to reside. The sample frequency sets the limit on the highest-frequency signals we can detect according to the Nyquist-Shannon Sampling Theorem. The duration of the sampling sets our frequency resolution– more sample time gives higher resolution. Five minutes of sampling at the maximum rate of 51.2 kSamples/s produces 245 MB of data. I added a 1TB hard drive to the Raspberry Pi so that it can easily store hours' worth of data. Figures 5 and 6 describe the readout system. We use the Valon 5009 frequency synthesizer. This model generates sine waves between 25 MHz and 6 GHz in 10 kHz increments. The increments must be small

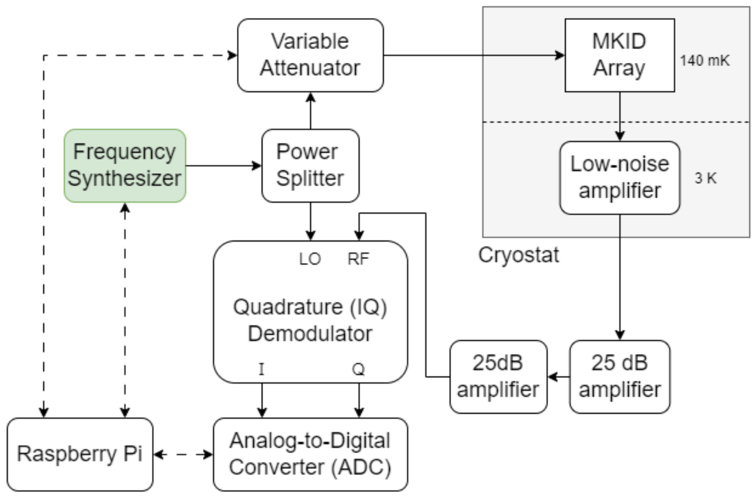

Figure 5: Schematic of the homodyne readout system. First, the frequency synthesizer (green for emphasis) generates a sinusoidal "probe tone" which is sent to the power splitter. The power splitter sends half of the power to the LO input of the quadrature demodulator. This is the "original" signal that will be compared to the output of the MKID array. The other output of the power splitter goes to a variable attenuator. The output of the attenuator enters the cryostat and goes to the MKID array. The probe tone leaves the MKID array and is amplified inside the cryostat by the low-noise amplifier, and again outside the cryostat by the 25dB amplifiers. The amplified signal is then sent to the RF port of the demodulator. The demodulator multiplies the LO and RF signals to determine their amplitude and phase difference. The IQ demodulator outputs the result through the "I" and "Q" ports. The analog-to-digital converter collects the I and Q output and digitizes it, so that it can be logged by the raspberry pi. The raspberry pi is used to control and monitor the ADC, the frequency synthesizer, and the variable attenuator.

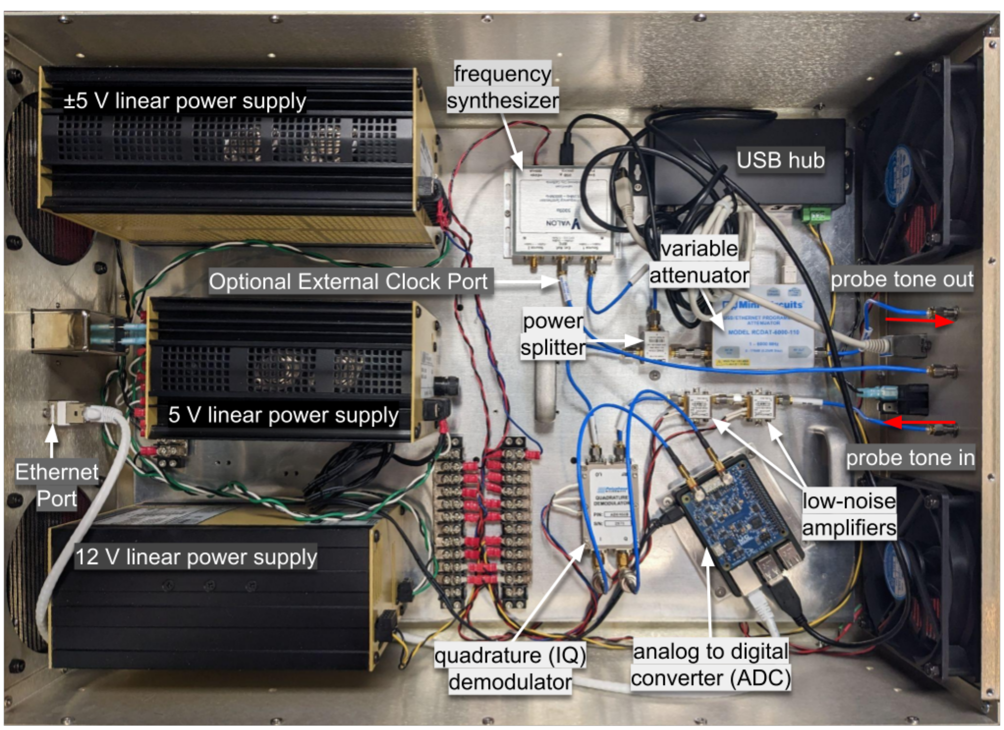

Figure 6: Photograph of the homodyne readout system. The ADC is mounted on top of a Raspberry Pi. The Raspberry Pi connects to the frequency synthesizer and the variable attenuator via the USB hub. The frequency synthesizer can optionally be operated with an external clock to improve the phase stability.

enough to resolve the widths of the resonance peaks (see tests 1, 2 in section 2.4). We use the Polyphase AD0460B Quadrature (IQ) demodulator. The signals into the LO and RF ports of the IQ demodulator should each be about 0 dBm. A Minicircuits ZFRSC-123-S+ power splitter sends a reference signal to LO. The other output of the power splitter must be attenuated further before it reaches the MKID array to avoid driving the detectors out of their operational range. We use the RCDAT-6000-110 programmable attenuator to tune the power sent to the MKID array. We amplify the return signal from the cryostat so that the input to the RF port of the quadrature demodulator is also 0 dBm. The output of the IQ demodulator goes to an analog-to-digital converter so that the data can be recorded on a computer. We use the MCC 172 two-channel DAQ HAT, which is mounted on a raspberry pi. The raspberry pi collects and records the data. The power supplies convert 60Hz/110V AC input to DC output. Using linear power supplies is essential because they produce a cleaner signal than a switching power supply. Even so, the power spectral density plots include a line at 60 Hz and its harmonics from the AC frequency, as expected. (See Fig. 8.)

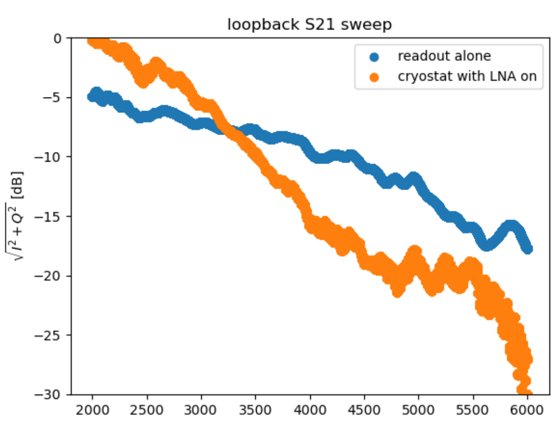

Figure 7: The blue line shows a loopback test where the cryostat was bypassed entirely, and the orange line shows a test bypassing only the detector module

Software The variable attenuator and frequency synthesizer come with user interfaces based on serial commands to the command prompt. I wrote a user interface to controls the attenuator, frequency synthesizer, and ADC in a single program. The user chooses the data collection mode and specifies relevant parameters such as attenuation, probe tone frequency, and sample rate. The UI then sends commands to the devices and starts collecting data from the ADC and storing it on the Raspberry Pi.

3 Methods: Readout System Validation

I have tested the readout system to verify that the performance is reliable and ready for detector testing. The tests were configured so that the output of the variable attenuator entered the cryostat, bypassed the MKID array, and went directly to the low-noise amplifier (Figure 5). This allows us to test as much of the system as possible before introducing the detectors.

3.1 Frequency Sweeps

We want to verify that the forward transmission, $|S_{21}|^2$ varies slowly with frequency. The S_{21} parameter measures the power received at port 2 from port 1; i.e. how much power is transmitted through the system. We measure S_{21} using the outputs of the IQ demodulator, such that

$$|S_{21}|^2 = I^2 + Q^2. \tag{3}$$

Using my readout system and UI, I swept the probe tone frequency from 2-4 GHz in increments of 200 kHz.

3.2 Noise spectra

We also need to examine the noise present in the system. We take the power spectral density (PSD) of the time-series data so that we can examine its properties in frequency space. The first step was to establish a reference and normalize the time-series data. I took one hour of data with the variable attenuator set to 35 dB, which is the required attenuation to get 0 dBm at the RF port. Then, I took another hour of data with the variable attenuator set to the maximum value, 110 dB. I Subtracted the average signal at 110 dBm (”off”) from the signal at 35 dBm (”on”) to establish a zero-point reference, and then divided by the average difference to scale the ”on” signal to 1 (unitless).

I took the FFT of the time-series data to calculate the power spectrum. Then, I calculated the PSD in units of dBc/Hz using

$$10 \times \log_{10}(\mathrm{PS} * N/F_s) \tag{4}$$

where PS is the power spectrum, N is the number of samples, and F_s is the sampling frequency. One hour of “on” (35dB attenuation) data was collected, followed by one hour of “off” (110 dB attenuation). Data collection was split into 5-minute increments. The probe tone was set to 3 GHz. The sample frequency was 51.2 kS/s and there were 30.1 million samples.

4 Results

4.1 Frequency sweeps

The frequency sweeps showed that the S_{21} transmission varied slowly with frequency. The requirement is that the transmission be smooth and varying slowly over the width of a resonance peak, which we expect to be a few MHz. The requirement is satisfied.

4.2 Noise Spectra

The PSD rises reasonably slowly with decreasing frequency, which should be acceptable for our measurements. A line at 60 GHz and its harmonics can clearly be seen

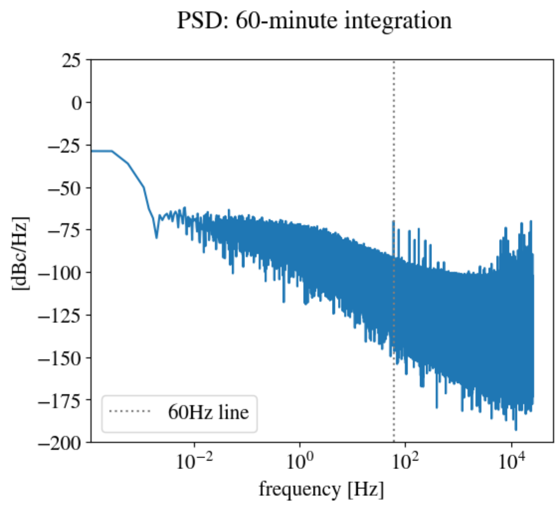

Figure 8: Plot of the noise spectrum loopback test with a 3GHz probe tone. The gray dotted line at 60 Hz is showing the expected contaminating noise from the 60 Hz AC power.

in the PSD. This is expected, and it is conventional to mask those channels. A variety of other lines are seen at high frequencies above about 10^3. We suspected the probe tone might have been aliased down. However, those same lines appeared for a variety of probe tone frequencies so this seems unlikely. The lines are at a high enough frequency that they should not interfere with testing the detectors, so we can proceed.

5 Conclusions

The readout system performs as designed, and meets the necessary criteria to move forward with detector characterization. The S21 sweep showed that the forward power transmission varied sufficiently slowly with frequency to characterize each resonator. The Noise spectrum measurement showed that the overall system noise was low and that the 1/f knee was at a sufficiently low frequency. The readout system has been tested and validated, and we can now commence detector characterization measurements.

References

[1] Raphael Flauger, J. Colin Hill, and David N. Spergel. Toward an understanding of foreground emission in the BICEP2 region. *Journal of Cosmology and Astroparticle Physics*, 2014(8), 8 2014.

[2] Brandon S. Hensley, Susan E. Clark, Valentina Fanfani, Nicoletta Krachmalnicoff, Giulio Fabbian, Davide Poletti, Giuseppe Puglisi, Gabriele Coppi, Jacob Nibauer, Roman Gerasimov, Nicholas Galitzki, Steve K. Choi, Peter C. Ashton, Carlo Baccigalupi, Eric Baxter, Blakesley Burkhart, Erminia Calabrese, Jens Chluba, Josquin Errard, Andrei V. Frolov, Carlos Hervías-Caimapo, Kevin M. Huffenberger, Bradley R. Johnson, Baptiste Jost, Brian Keating, Heather McCarrick, Federico Nati, Mayuri Sathyanarayana Rao, Alexander van Engelen, Samantha Walker, Kevin Wolz, Zhilei Xu, Ningfeng Zhu, and Andrea Zonca. The Simons Observatory: Galactic Science Goals and Forecasts. 11 2021.

[3] B. R. Johnson, D. Flanigan, M. H. Abitbol, P. A.R. Ade, S. Bryan, H. M. Cho, R. Datta, P. Day, S. Doyle, K. Irwin, G. Jones, D. Li, P. Mauskopf, H. McCarrick, J. McMahon, A. Miller, G. Pisano, Y. Song, H. Surdi, and C. Tucker. Development of Multi-chroic MKIDs for Next-Generation CMB Polarization Studies. *Journal of Low Temperature Physics*, 193(3-4):103–112, 11 2018.

[4] Justin Lazear, Peter A. R. Ade, Dominic Benford, Charles L. Bennett, David T. Chuss, Jessie L. Dotson, Joseph R. Eimer, Dale J. Fixsen, Mark Halpern, Gene Hilton, James Hinderks, Gary F. Hinshaw, Kent Irwin, Christine Jhabvala, Bradley Johnson, Alan Kogut, Luke Lowe, Jeff J. McMahon, Timothy M. Miller, Paul Mirel, S. Harvey Moseley, Samelys Rodriguez, Elmer Sharp, Johannes G. Staguhn, Eric R. Switzer, Carole E. Tucker, Amy Weston, and Edward J. Wollack. The Primordial Inflation Polarization Explorer (PIPER). 7 2014.

[5] H. McCarrick, G. Jones, B. R. Johnson, M. H. Abitbol, P. A.R. Ade, S. Bryan, P. Day, T. Essinger-Hileman, D. Flanigan, H. G. Leduc, M. Limon, P. Mauskopf, A. Miller, and C. Tucker. Design and performance of dual-polarization lumped-element kinetic inductance detectors for millimeter-wave polarimetry. *Astronomy and Astrophysics*, 610, 2 2018.

[6] Michael J. Mortonson and Uroš Seljak. A joint analysis of Planck and BICEP2 B modes including dust polarization uncertainty. *Journal of Cosmology and Astroparticle Physics*, 2014(10), 10 2014.

[7] Suzanne Staggs, Jo Dunkley, and Lyman Page. Recent discoveries from the cosmic microwave background: A review of recent progress, 2 2018.